Supporting Information

Checco et al. 10.1073/pnas.1420380112

SI Methods

Materials. Protected α-amino acids and benzotriazole-1-yl-oxy-tris-pyrrolidino-phosphonium hexafluorophosphate (PyBOP) were purchased from Novabiochem and Chem-Impex International. Protected β^3-amino acids were purchased from Chem-Impex International and PepTech Corporation. Fmoc-ACPC-OH was purchased from Chem-Impex International (15073). Fmoc-APC(Boc)-OH was synthesized as previously described (1). NovaPEG Rink Amide resin was purchased from Novabiochem (855047). All other solvents and reagents used for peptide synthesis were purchased from Sigma-Aldrich or Fisher Scientific.

Peptide Synthesis and Purification. α-Peptides were synthesized on NovaPEG Rink Amide resin either on solid phase using a Symphony automated peptide synthesizer (Protein Technologies) as previously reported (2) or synthesized using microwave-assisted solid-phase conditions, as described below. Z-VEGF was synthesized on a Symphony automated peptide synthesizer, double coupling each amino acid, as previously described (3). Z-TNFα was synthesized in the same manner as Z-VEGF. α/β-Peptides were synthesized on NovaPEG Rink Amide resin using microwave-assisted solid-phase conditions (4) based on Fmoc protection of the main chain amine. Coupling reactions were carried out by treating the resin with a solution of protected amino acid, activated with PyBOP and 0.1 M 1-hydroxybenzotriazole (HOBt) in the presence of *N*,*N*-diisopropylethylamine (DIEA) in 1-methyl-2-pyrrolidone (NMP). Deprotection of the Fmoc protecting group was carried out using a solution of 5% piperazine, 0.1 M HOBt in *N*,*N*-dimethylformamide (DMF). All oligomers have a free amine at their N terminus, except for the BODIPY-labeled BODIPY-v114*$_{\Delta NT}$ described below. After the completion of the synthesis, α- and α/β-peptides containing no cysteine or methionine residues were cleaved from the resin using a solution of 95% trifluoroacetic acid (TFA), 2.5% H_2O, and 2.5% triisopropylsilane (TIS). α- and α/β-peptides containing cysteine or methionine residues were cleaved from the resin using a solution of 94% TFA, 2.5% H_2O, 2.5% 1,2-ethanedithiol, and 1% TIS. Excess TFA was removed under a stream of nitrogen, and the crude peptides were precipitated by the addition of cold diethyl ether. For α- and α/β-peptides without a disulfide bond, solutions of crude peptide were purified by reverse-phase HPLC. For α- and α/β-peptides containing a disulfide bond, crude ether-precipitated peptides were dissolved in dimethyl sulfoxide (DMSO) (~10 mL for 50-μmol synthesis), and ammonium hydroxide (NH_4OH) was added to make the solution basic (~25 drops for 50-μmol synthesis). These DMSO solutions were exposed to air, and the oligomers allowed to oxidize over the course of 4–7 d, followed by purification by HPLC. Final purity was assessed by analytical HPLC and identity confirmed by MALDI-TOF-MS. All oligomers used in this study are believed to be ≥95% pure as determined by analytical HPLC, except for those explicitly stated otherwise in Fig. S1 *E* and *F*. Calculated (calc.) and observed (obs.) masses of purified oligomers, as determined by MALDI-TOF-MS (monoisotopic $[M+H]^+$, *m*/*z*), are as follows: Z-VEGF: calc. = 6,661.4, obs. = 6,660.5; Z-VEGF(1–38): calc. = 4,486.2, obs. = 4,486.5; α-VEGF-1: calc. = 4,417.2, obs. = 4,417.7; α-VEGF-2: calc. = 4,484.2, obs. = 4,484.8; α/β-VEGF-1: calc. = 4,585.3, obs. = 4,585.4; α/β-VEGF-2: calc. = 4,542.3, obs. = 4,541.8; α/β-IgG-1: calc. = 4,620.3, obs. = 4,619.9; α/β-IgG-2: calc. = 4,622.3, obs. = 4,621.9; Z-TNFα: calc. = 6,473.4, obs. = 6,474.6; α/β-TNFα-1: calc. = 4,400.3, obs. = 4,399.8; α/β-TNFα-2: calc. = 4,474.3, obs. = 4,473.6; BODIPY-v114*$_{\Delta NT}$: calc. = 2,613.2, obs. = 2,612.8; VEGF-S1: calc. = 4,581.2, obs. = 4,580.9; VEGF-S2: calc. = 4,567.2, obs. = 4,567.5; VEGF-S3: calc. = 4,593.2, obs. = 4,593.2; VEGF-S4: calc. = 4,593.2, obs. = 4,593.4.

Protein Expression and Purification. $VEGF_{165}$ was expressed and purified as previously reported (5).

The gene encoding for the receptor-binding domain of human VEGF, residues 8–109, was subcloned from a pET-3d vector containing the gene for $VEGF_{165}$, residues 2–165 (forward primer: 5′-GTTCCATGGGGCAGAATCATCAC-3′; reverse primer: 5′-GGCGGATCCTCATCATCAATCTTTCTTT-3′). Sanger DNA sequencing confirmed the presence of the $VEGF_{8–109}$ gene in a pET-3d vector. *Escherichia coli* BL21(DE3)-RIPL cells (Stratagene; 230280) were transformed with the pET-3d vector containing the $VEGF_{8–109}$ gene using heat-shock transformation method. Cells were grown at 37 °C in LB media supplemented with 50 μg/mL carbenicillin and 25 μg/mL chloramphenicol. $VEGF_{8–109}$ expression was induced with 0.4 mM isopropyl β-D-1-thiogalactopyranoside (IPTG) at an OD_{600} of ~0.6, and cells were grown for an additional 3 h. The cells were pelleted by centrifugation at 3,000 × *g* for 30 min at 4 °C, washed with Tris-buffered saline (20 mM Tris·HCl, 150 mM NaCl, pH 7.5), and pelleted by centrifugation at 3,000 × *g* for 30 min at 4 °C.

Protocol for the isolation and refolding of $VEGF_{8–109}$ was adapted from Peterson et al. (5). Isolated inclusion bodies were solubilized in 27 mL of dissolving buffer (20 mM Tris·HCl, 7.5 M urea, 20 mM DTT, pH 7.5) overnight at 4 °C. Solubilized inclusion bodies were clarified by centrifugation. Unfolded and reduced $VEGF_{8–109}$ was diluted in dissolving buffer to 0.75 mg/mL and dialyzed extensively against refolding buffer (20 mM Tris·HCl, 400 mM NaCl, 1 mM cysteine, pH 8.4) at 4 °C. Purity of the $VEGF_{8–109}$ homodimer was confirmed by SDS/PAGE and analytical reverse-phase HPLC with a final yield of ~48 mg/L for a 3-L expression. A portion of the refolded $VEGF_{8–109}$ dimer was dialyzed against PBS for direct binding fluorescence polarization (FP) assays to validate activity (protocol given below). The tracer in this assay has a dissociation constant (K_D) of 21 nM against $VEGF_{165}$. The K_D determined for the refolded $VEGF_{8–109}$ dimer was 14 nM. These data suggest that $VEGF_{8–109}$ is correctly folded and is able to bind the tracer peptide with essentially the same affinity as $VEGF_{165}$. For cocrystallization screens, $VEGF_{8–109}$ was dialyzed against crystallization buffer (20 mM Tris·HCl, 150 mM NaCl, pH 7.5) and concentrated to ~500 μM, as determined by UV absorbance using an extinction coefficient of 12,920 $M^{-1}\cdot cm^{-1}$ for the $VEGF_{8–109}$ dimer, as determined by ExPASy Server (6).

VEGF FP Assays. Inhibitors of the $VEGF_{165}$–VEGFR interaction were evaluated using our $VEGF_{165}$ direct-binding and competition FP assays, as previously described (5). The tracer used in the assays reported here was the Met→norleucine variant of the previously reported tracer [peptide BODIPY-v114*$_{\Delta NT}$, sequence (BODIPY^{TMR})-X-CDIHV(Nle)WEWECFERL-NH_2, X = [2-(2-amino-ethoxy)-ethoxy]acetic acid, (Nle) = norleucine, where cysteines are linked in intramolecular disulfide; K_D = 21 nM]. To account for slight variations in amount of active protein resulting from each expression, the K_D for BODIPY-v114*$_{\Delta NT}$ was measured for each $VEGF_{165}$ expression stock by direct-binding FP assay, and the resulting K_D value was used for the determination of inhibitor dissociation constant (K_i) values derived from competition FP assays using that stock. DMSO stock solutions of α- and α/β-peptide inhibitors were prepared, and concentration

was determined by UV absorbance at 280 nm. Extinction coefficients for α- and α/β-peptides were calculated based on the number of tryptophan residues ($\varepsilon_{280} = 5{,}690\ M^{-1}{\cdot}cm^{-1}$), tyrosine residues ($\varepsilon_{280} = 1{,}280\ M^{-1}{\cdot}cm^{-1}$), and cystines ($\varepsilon_{280} = 120\ M^{-1}{\cdot}cm^{-1}$) in each primary sequence (7). Competition FP assays were performed by adding 2 μL of serial dilutions of inhibitor in DMSO to 48 μL of solution containing BODIPY-v114*$_{\Delta NT}$ (final concentration, 10 nM) and $VEGF_{165}$ (final concentration, 40 nM) in FP buffer (50 mM NaCl, 16.2 mM Na_2HPO_4, 3.8 mM KH_2PO_4, 0.15 mM NaN_3, 0.15 mM EDTA, 0.5 mg/mL Pluoronic-F68, pH 7.5) in 384-well, black polystyrene plates (Costar). Plates were incubated at room temperature for 5–7 h, and then read on a BioTek Synergy 2 microplate reader. Each condition was run in duplicate in each assay. Inhibition constants (K_i) were determined from FP data using methods described for a competitive binding model with GraphPad Prism 4.0 (5, 8). Fig. S1 shows representative competition FP assays for each of the reported oligomers.

CD Spectroscopy. CD measurements (Fig. S2) were performed on an Aviv Model 420 CD Spectrometer. Solutions of α- and α/β-peptides (75 μM) were prepared in PBS, pH 7.5. Spectra were collected at 20 °C in a 0.1-cm quartz cell with a wavelength step size of 1 nm and a 10-s averaging time. Spectra were normalized to units of [θ] (degrees square centimeter per decimole residue, deg cm^2 $dmol^{-1}$ res^{-1}) × 10^{-3} using the exact concentration determined by UV absorbance (see above) to account for slight variations in concentration between solutions.

Crystallization. Crystallization screens were carried out by premixing a solution of $VEGF_{8–109}$ dimer in crystallization buffer with a stock of α/β-VEGF-1 in water ($VEGF_{8–109}$ final concentration, 200 μM; α/β-VEGF-1 final concentration, 640 μM). After 40 min at room temperature, the protein+α/β-peptide solution was briefly centrifuged, and then drops of 1 μL of the protein+α/β-peptide mixture with 1 μL of each precipitate condition from the Hampton Index (Hampton Research; HR2-144) were suspended over a 300-μL reservoir in 48-well crystallization trays. Optimized crystallization conditions were based on Index condition 92 and grew reliably at various concentrations of protein+α/β-peptide. Importantly, crystals from condition 92 did not grow with $VEGF_{8–109}$ alone, suggesting the presence of the $VEGF_{8–109}$+α/β-VEGF-1 complex in the crystal. The final conditions were droplets of 1 μL of 110 μM $VEGF_{8–109}$ and 340 μM α/β-VEGF-1 (premixed for 3 h) with 1 μL of 0.1 M magnesium formate dihydrate, 15% (wt/vol) PEG3350, 30% (vol/vol) glycerol over 300-μL reservoir solution in a 48-well crystallization tray. The addition of 30% (vol/vol) glycerol in the optimized conditions was desired as a cryoprotectant. Crystals grew over the course of several days.

X-Ray Data Collection and Structure Determination. Crystals were vitrified directly in liquid nitrogen on a nylon loop. Diffraction data were collected at the Life Sciences Collaborative Access Team beamline 21-ID-F at the Advanced Photon Source (APS), Argonne National Laboratory. A total of 180 1° oscillation images with 8-s exposure time was collected. Data were indexed, integrated, scaled, and merged with the programs *XDS* and *XSCALE* (9). Data were truncated at 3.1-Å resolution due to extreme anisotropy (Fig. S4*B*). A molecular replacement solution was found with the program *Phaser* using polyalanine backbones of the $VEGF_{8–109}$ dimer (coordinates extracted from PDB ID code 3S1K) and the two-helix analog of Z-IgG (PDB ID code 1ZDD) as search models (*TFZ* = 9.5; *LLG* = 856) (10). Anisotropic scaling and refinement were carried out in the program *phenix.refine* (11, 12) in combination with manual real-space model building and refinement in the program *Coot* (Crystallographic Object-Oriented Toolkit) (13). The initial refinement strategy comprised a combination of rigid-body refinement (14) and simulated annealing of torsion angles; intermediate rounds of refinement comprised coordinate, group atomic displacement parameter (ADP), and TLS refinement; final rounds of refinement comprised coordinate, group ADP, and TLS refinement with optimized ADP and coordinate weights. A composite omit map generated with the function *phenix.composite_omit_map* and simulated torsion annealing indicated weak electron density around each α/β-VEGF-1 disulfide bond, presumably due to radiation damage. A composite omit map generated from data collected in the first 120° showed increased density around each α/β-VEGF-1 disulfide bond relative to the final model. Due to this radiation damage, sulfur occupancies were also refined in each α/β-VEGF-1 disulfide bond during the final round of refinement. Eighteen TLS groups were assigned with the function *phenix.find_tls_groups* in *phenix.refine*. Residues 1–7 of each α/β-VEGF-1 molecule (chains C and D); residues 8–12, 108–109 for chain A; and residues 8–13, 107–109 of chain B were not modeled due to lack of electron density. For 34 residues within the structure (primarily within the loop regions and termini of $VEGF_{8–109}$ and the last two turns of the α/β-peptide C-terminal helix), side chains were not modeled in due to a lack of supporting electron density. Noncrystallographic symmetry restraints were applied to torsion angles; secondary structure restraints and Ramachandran restraints were also applied to the model (15). Standard peptide bond geometries were used to define custom restraints for links between α- and β-amino acid residues. In addition to these custom link restraints, the slack parameter feature in *phenix.refine* was used to define hydrogen bond restraints of 2.9 ± 0.2 Å corresponding to helical secondary structure in α/β-VEGF-1. Figures depicting high-resolution structures were prepared using PyMOL molecular visualization software.

Proteinase K Susceptibility Assay. Stock solutions of 50 μg/mL proteinase K (Novagen; 70663-4) were prepared in Tris-buffered saline (TBS), pH 7.5. Solutions of 90 μM α-peptide or α/β-peptide in TBS were prepared, as determined by UV absorbance (see above). For each proteolysis reaction, the α- or α/β-peptide stock was diluted with TBS to achieve a final concentration of 45 μM. Proteinase K stock was added (final concentration, 10 μg/mL), and the reaction proceeded at room temperature. For each time point, 50 μL of the reaction mixture was removed and quenched by the addition of 100 μL of 1:1 H_2O/acetonitrile with 1% TFA. A volume of 125 μL of the resulting quenched solution was injected onto analytical reverse-phase HPLC. The relative amount of peptide remaining was quantified by integration of the peak at 220 nm in a series of HPLC chromatograms. Each reaction was run at least in duplicate. Half-lives were determined by fitting the time course of peptide degradation to an exponential decay model using GraphPad Prism 4.0 (Fig. S5).

Human Umbilical Vein Endothelial Cell Proliferation Assay. Stock solutions of α- or α/β-peptide in PBS were prepared at a concentration of 200 μM, as determined by UV absorbance. PBS stocks were sterile filtered through 0.2-μm syringe filters before determining concentration. These PBS stocks of α- and α/β-peptides were stored at −20 °C between experiments and were used within ∼1 mo, attempting to minimize freeze/thaw cycles. Human umbilical vein endothelial cells (HUVECs) (Lonza; CC2519) were cultured using Medium 199 (M199) (Mediatech; 50-050-PB) supplemented with penicillin/streptomycin (HyClone; SV30010) and EGM-2 (Lonza; CC4176) at 37 °C in 5% CO_2. Cells were grown to 60–80% confluence before beginning an experiment. On day 0 of experiments, cells were serum-starved in Serum Starvation medium, consisting of M199 with 2 vol% cosmic calf serum (HyClone; SH30087), overnight. On day 1 of experiments, cells were trypsinized and reseeded in gelatin-coated 96-well plates at a density of 3,000–4,000 cells per well in Serum Starvation medium and allowed to attach for 6–8 h. Appropriate dilutions of

α- or α/β-peptide were made with PBS, and the resulting solutions were premixed with recombinant human $VEGF_{165}$ (R&D Systems; 293-VE-010) or recombinant human FGF basic (FGF-2) (R&D Systems; 233-FB-025) in Serum Starvation medium and incubated at room temperature for ∼1 h. For controls with no inhibitor, the same amount of PBS was preincubated with growth factor alone. After preincubation, these solutions were then added to the cells to give a final concentration of 10 ng/mL growth factor (except in "no growth factor" controls), between 0 and 50 μM peptide, and 25 vol% PBS. Cells were then cultured in the presence/absence of inhibitors and/or growth factor for 36 h. Relative cell proliferation was quantified using the Click-iT EdU Alexa Flour 488 Assay (Life Technologies; C10337). After 24 h of exposure to assay conditions (on day 2), EdU was added (final concentration, 10 μM), and the cells were maintained at 37 °C in 5% CO_2 for an additional 12 h (36 h total) before being fixed with 10% buffered formalin. EdU incorporation was detected using Life Technologies' assay protocol. All cell nuclei were counterstained with the Hoechst 33342 stain supplied with the Click-iT EdU assay kit (1:1,000 dilution in PBS), and proliferating cells containing incorporated EdU were stained using copper-catalyzed alkyne-azide click addition of Alexa Fluor 488. Plates were imaged using a Nikon Ti-Eclipse inverted epifluorescence microscope with filters for FITC (detecting Alexa Fluor 488, EdU-labeled cells) and DAPI (detecting Hoechst 33342, labeling all cells). Images were analyzed using NIS-Elements, Version 3.2, AR Imaging Software to count the number of proliferating cells (EdU stained) and total number of cells (Hoechst stained).

Data presented in the main text figure (Fig. 4) represent the mean ± SD of relative proliferation collected from eight independent experiments. Because the maximum level of VEGF-induced proliferation varied for each independent experiment, each experimental condition was normalized to the relative "No-inhibitor" ($VEGF_{165}$ only) control in its respective experiment (10 ng/mL $VEGF_{165}$ in Serum Starvation medium with 25 vol% PBS with no inhibitor present). For statistical analysis, a two-tailed ratio *t* test on the logarithmically transformed ratios was used to determine if the mean ratio for a given experimental condition differed from 1.0 (the No-inhibitor control). To avoid false positives from making multiple comparisons, we used the Bonferroni correction to set a stricter significance threshold and require a given value of $P \leq 0.05/5 = 0.01$ for statistical significance.

Data presented in Fig. S6 *B* and *C* are representative experiments where values represent the mean ± SD for replicate wells on a given plate, and the value for each well is normalized relative to the average value of proliferating cells in the No-inhibitor ($VEGF_{165}$-only) condition. A two-tailed *t* test comparing the experimental conditions to control conditions on logarithmically transformed values was used to determine statistical significance. As above, we used the Bonferroni correction to determine our significance threshold as a value of $P \leq 0.0125$ for Fig. S6*B* and $P \leq 0.0055$ for Fig. S6*C*.

LIVE/DEAD Viability Assay. HUVECs were cultured and treated with inhibitors and $VEGF_{165}$, as described above. After 36 h in culture under the experimental conditions, cells were stained using LIVE/DEAD Viability/Cytotoxicity kit (Life Technologies; L3224). Calcein AM (4 μM) and ethidium homodimer-1 (2 μM) in M199 without serum were added to cells for 30 min at 37 °C in 5% CO_2 to stain live and dead cells, respectively. After 30-min incubation with staining reagents, the medium was removed from wells and replaced with fresh M199 for imaging. Plates were imaged as above using filters for FITC (detecting calcein-AM, live cells) and Texas Red (detecting ethidium homodimer-1, dead cells). Images were analyzed using NIS-Elements, Version 3.2, AR Imaging Software to count the number of live and dead cells. The fraction of live cells was determined by dividing the number of live stained cells by the total number of cells (live stained cells + dead stained cells) (Fig. S6*A*). Data were analyzed using a two-tailed *t* test to determine statistical significance; all conditions displayed a value of $P > 0.05$.

Human IgG1-κ ELISA. The binding of α/β-peptides to human IgG1-κ was determined by indirect and competition ELISA. α/β-IgG-1 and α/β-IgG-2 were each conjugated to BSA by dissolving ∼1 mg of purified α/β-peptide in a solution containing 3% BSA, 8 mM glutaraldehyde in 0.1 M NaOAc, pH 7.0, at a total volume of 330 μL. The conjugation reaction was allowed to proceed on a rocker at room temperature for 2 h and quenched by the addition of 5–6 mg of glycine and additional incubation for 1 h. After quenching, the reaction solution was diluted to 3 mL with PBS, pH 7.0, and dialyzed overnight into PBS at 4 °C using 10,000 MWCO dialysis membrane. After dialysis, the α/β-peptide+BSA conjugates were concentrated to ∼500 μL using 10,000 MWCO Amcon Ultra-15 centrifugal filter units (EMD Millipore; UFC901024). These concentrated solutions were stored at −20 °C, diluted, and used directly for indirect and competition ELISA experiments.

For indirect ELISA, 50 μL of serial dilutions (starting with 1:50 dilution in PBS, pH 7.4) of α/β-IgG-1 or α/β-IgG-2 conjugated to BSA were immobilized onto a Nunc clear polystyrene 96-well ELISA plate (Thermo Scientific; 430341) in PBS, incubated overnight at 4 °C. After immobilization, the plate was washed with PBS plus 0.05% Tween 20 (for this and all subsequent washes, wells were rinsed three to five times with 200 μL of PBS plus 0.05% Tween) and blocked with 1% BSA in PBS plus 0.05% Tween for 1–2 h at room temperature. The plate was then washed with PBS plus 0.05% Tween and 100 μL of human IgG1-κ (Sigma; I5154) was added and incubated at room temperature for 1.5 h. Because a stronger signal was observed for the α/β-IgG-2+BSA conjugate relative to the α/β-IgG-1+BSA conjugate (possibly due to a difference in affinity or in conjugation efficiency), 30 μg/mL human IgG1-κ in PBS plus 0.05% Tween was used for assays in which α/β-IgG-1 was immobilized and 10 μg/mL human IgG1-κ in PBS plus 0.05% Tween was used for assays in which α/β-IgG-2 was immobilized. After immobilized α/β-peptide was allowed to bind human IgG1-κ, the plate was washed with PBS plus 0.05% Tween and the binding of human IgG1-κ detected by adding 100 μL of 1:2,000 dilution of goat anti-human IgG (Fab-specific)-alkaline phosphatase antibody (Sigma; A8542) and incubating at room temperature for 1 h. After washing with PBS plus 0.05% Tween, 50 μL of SIGMA*FAST* *p*-nitrophenyl phosphate (*p*NPP) solution (Sigma; N1891) was added to each well, and the alkaline phosphatase reaction was allowed to proceed at room temperature. Plates were read during the time course of the reaction on a BioTek Synergy 2 microplate reader, reading absorbance at 405 nm (Fig. S7 *A* and *B*). Each condition was run in duplicate. As a control, no increase in signal over background was observed in wells in which no α/β-peptide was immobilized. In addition, no signal was observed for either immobilized α/β-peptide when no human IgG1-κ was incubated, indicating that the goat anti-human IgG (Fab-specific)-alkaline phosphatase antibody does not bind nonspecifically to the α/β-peptides or BSA.

For competition ELISA, 50 μL of a 1:100 dilution of the α/β-IgG-2+BSA conjugate in PBS was immobilized onto the ELISA plate and incubated at 4 °C overnight. After immobilization, the plate was washed with PBS plus 0.05% Tween, blocked with 1% BSA for 1–2 h, and then washed with PBS plus 0.05% Tween. Serial dilutions of soluble α/β-peptides in DMSO were prepared (final concentrations, 27 nM to 60 μM), and 10 μL of each of these solutions added to 240 μL of human IgG1-κ (final concentration, 10 μg/mL) in PBS plus 0.05% Tween. The soluble α/β-peptides were allowed to preincubate with human IgG1-κ for 1–2 h, and then 100 μL of each α/β-peptide+IgG1-κ mixture was added to the ELISA plate and incubated at room temperature for 2 h. The binding of human IgG1-κ to the immobilized α/β-IgG-2 was measured using goat anti-human IgG (Fab-specific)-alkaline

phosphatase antibody, as described above. Each condition was run in duplicate. Plates were read during the time course of the reaction on a BioTek Synergy 2 microplate reader, reading absorbance at 405 nm. Reactions were quenched with the addition of 100 μL of 1 M NaOH to each well. To compare the ability of each soluble α/β-peptide to bind human IgG1-κ and inhibit binding to the immobilized α/β-IgG-2, IC_{50} values were calculated by fitting the ELISA absorbance data to a sigmoidal dose–response equation using GraphPad Prism 4.0 (Fig. S7 *C* and *D*).

TNFα–TNFR Competition ELISA. The binding of α/β-peptides to TNFα to inhibit the binding of TNFα to TNFR1 was determined by competition ELISA. For each competition ELISA experiment, 50 μL of 1 μg/mL recombinant human sTNF RI/TNFRSF1A (TNFR1) (R&D Systems; 636-R1-025) in PBS was added to each well and incubated at 4 °C overnight to immobilize TNFR1 onto the ELISA plate. After immobilization, the plate was washed with PBS plus 0.05% Tween, blocked with 1% BSA in PBS for 2–4 h, and then washed again with PBS plus 0.05% Tween. Serial dilutions of soluble α/β-peptides in DMSO were prepared (final concentrations, 0.036 nM to 10 μM), and 10 μL of each of these solutions added to 240 μL of recombinant human TNFα (R&D Systems; 210-TA-020; final concentration, 0.081 μg/mL) in PBS plus 0.05% Tween. The α/β-peptides were allowed to incubate with TNFα for 3 h, and then 100 μL of each α/β-peptide+TNFα mixture was added to wells on the ELISA plate and incubated at room temperature for 1 h. The plate was then washed with PBS plus 0.05% Tween, and the presence of TNFα was detected by adding 100 μL of 0.40 μg/mL human TNFα biotinylated antibody (R&D Systems; BAF210) in PBS plus 0.05% Tween and incubating at room temperature for 1 h. The plate was washed with PBS plus 0.05% Tween, and 100 μL of 1:1,000 dilution of streptavidin-alkaline phosphatase (R&D Systems; AR001) in PBS plus 0.05% Tween was added and allowed to incubate at room temperature for 30 min. After washing with PBS plus 0.05% Tween, 50 μL of SIGMA*FAST* *p*-nitrophenyl phosphate solution (Sigma; N1891) was added to each well, and the alkaline phosphatase reaction was allowed to proceed at room temperature. Plates were read during the time course of the reaction on a BioTek Synergy 2 microplate reader, reading absorbance at 405 nm. Each condition was run in duplicate. To compare the ability of each soluble α/β-peptide to inhibit the binding of TNFα to immobilized TNFR1, IC_{50} values were calculated by fitting the ELISA absorbance data to a sigmoidal dose–response equation using GraphPad Prism 4.0 (Fig. S8).

1. Lee HS, LePlae PR, Porter EA, Gellman SH (2001) An efficient route to either enantiomer of orthogonally protected *trans*-3-aminopyrrolidine-4-carboxylic acid. *J Org Chem* 66(10):3597–3599.
2. Lee EF, et al. (2011) Structural basis of Bcl-x_L recognition by a BH3-mimetic α/β-peptide generated by sequence-based design. *ChemBioChem* 12(13):2025–2032.
3. Fedorova A, et al. (2011) The development of peptide-based tools for the analysis of angiogenesis. *Chem Biol* 18(7):839–845.
4. Horne WS, Price JL, Gellman SH (2008) Interplay among side chain sequence, backbone composition, and residue rigidification in polypeptide folding and assembly. *Proc Natl Acad Sci USA* 105(27):9151–9156.
5. Peterson KJ, et al. (2008) A fluorescence polarization assay for identifying ligands that bind to vascular endothelial growth factor. *Anal Biochem* 378(1):8–14.
6. Gasteiger E, et al. (2005) Protein identification and analysis tools on the ExPASy server. *The Proteomics Protocols Handbook*, ed Walker JM (Humana, Totowa, NJ), pp 571–607.
7. Gill SC, von Hippel PH (1989) Calculation of protein extinction coefficients from amino acid sequence data. *Anal Biochem* 182(2):319–326.
8. Roehrl MH, Wang JY, Wagner G (2004) A general framework for development and data analysis of competitive high-throughput screens for small-molecule inhibitors of protein-protein interactions by fluorescence polarization. *Biochemistry* 43(51):16056–16066.
9. Kabsch W (2010) XDS. *Acta Crystallogr D Biol Crystallogr* 66(Pt 2):125–132.
10. McCoy AJ, et al. (2007) Phaser crystallographic software. *J Appl Cryst* 40(Pt 4):658–674.
11. Afonine PV, Grosse-Kunstleve RW, Adams PD, Urzhumtsev A (2013) Bulk-solvent and overall scaling revisited: Faster calculations, improved results. *Acta Crystallogr D Biol Crystallogr* 69(Pt 4):625–634.
12. Afonine PV, et al. (2012) Towards automated crystallographic structure refinement with *phenix.refine*. *Acta Crystallogr D Biol Crystallogr* 68(Pt 4):352–367.
13. Emsley P, Cowtan K (2004) Coot: Model-building tools for molecular graphics. *Acta Crystallogr D Biol Crystallogr* 60(Pt 12 Pt 1):2126–2132.
14. Afonine PV, Grosse-Kunstleve RW, Urzhumtsev A, Adams PD (2009) Automatic multiple-zone rigid-body refinement with a large convergence radius. *J Appl Cryst* 42(Pt 4):607–615.
15. Headd JJ, et al. (2012) Use of knowledge-based restraints in *phenix.refine* to improve macromolecular refinement at low resolution. *Acta Crystallogr D Biol Crystallogr* 68(Pt 4):381–390.

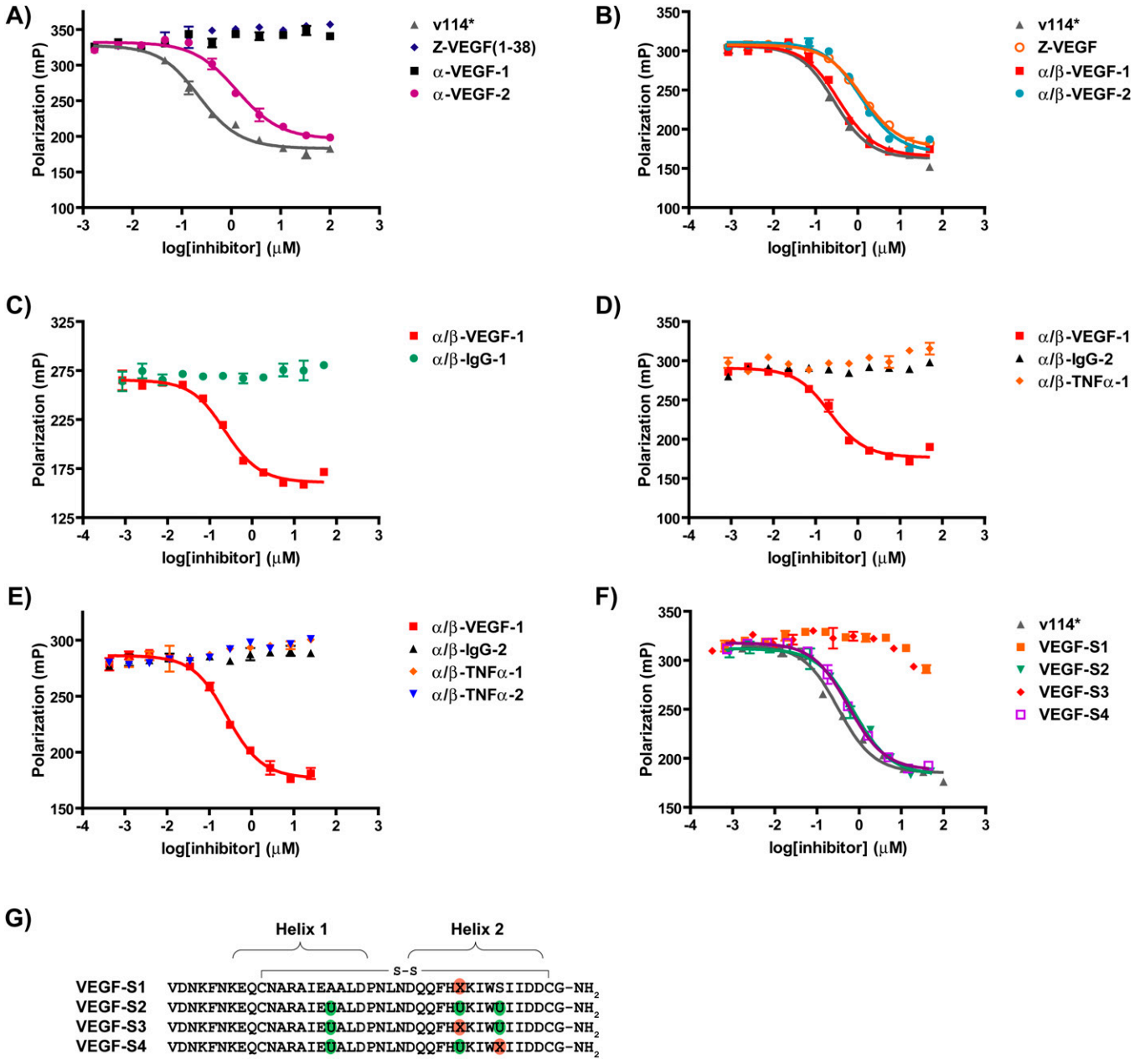

G)

Fig. S1. Representative $VEGF_{165}$ competition FP assays evaluating the binding of oligomers used in this study to $VEGF_{165}$. Each data point represents the mean ± SEM for duplicate wells on the plate. In *A*, *B*, and *F*, previously reported phage-derived peptide v114* (reported K_i = 0.060 μM) is used as a positive control (1). The K_i value for α/β-VEGF-1 reported in the main text (K_i = 0.11 μM) is derived from *B*, which directly compares v114*, Z-VEGF, α/β-VEGF-1, and α/β-VEGF-2. α/β-VEGF-1 is then used as a positive control in *C*–*E*. K_i values fit for each of these independent experiments ranges from 0.064 to 0.11 μM. This small variation highlights the variability we typically see in this FP assay with α/β-VEGF-1 or other active antagonists for fitted equilibrium constants between independent experiments. Note that, in *E*, the stock of α/β-TNFα-2 used in this experiment (but no other experiment using this compound) was only ∼90% pure by analytical HPLC, whereas all other oligomers used in this study (except for those described below) are ≥95% pure as determined by analytical HPLC. *F* shows representative $VEGF_{165}$ competition FP assay evaluating the binding of VEGF-S1 (K_i > 38.8 μM), VEGF-S2 (K_i = 0.23 μM), VEGF-S3 (K_i > 19.6 μM), and VEGF-S4 (K_i = 0.17 μM). These results show that the incorporation of cyclic β-residue ACPC (X) at position 30 was not tolerated, but Aib substitution at this position was well tolerated. Based on these results, we incorporated Aib also at a position in helix 1 near the loop (position 17) rather than a β-residue. Oligomers in *F* were >92% pure. *G* shows the sequences of the analogs in *F*, where colored circles indicate nonnatural residues as depicted in Fig. 2*B* in the main text, and cysteine residues are engaged in an intramolecular disulfide bond.

1. Haase HS, et al. (2012) Extending foldamer design beyond α-helix mimicry: α/β-Peptide inhibitors of vascular endothelial growth factor signaling. *J Am Chem Soc* 134(18):7652–7655.

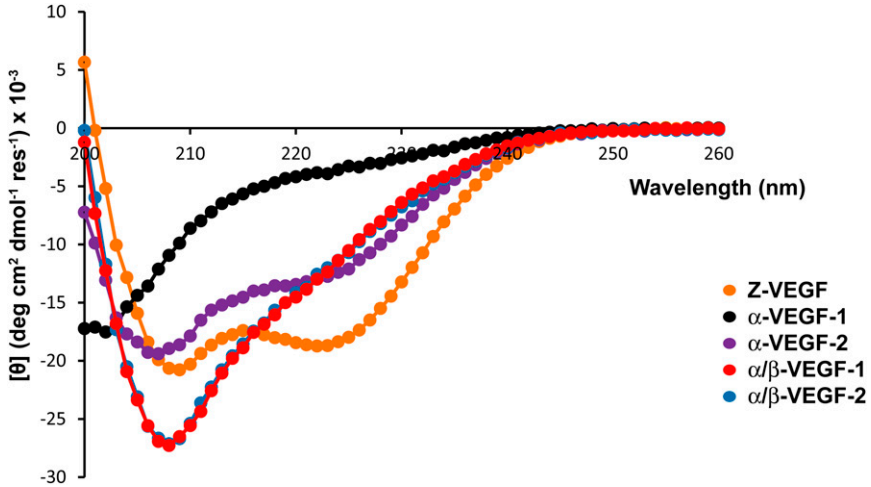

Fig. S2. Far-UV CD data for α- and α/β-peptides targeting VEGF based on Z-VEGF. All oligomers 75 μM in PBS, pH 7.5, 20 °C.

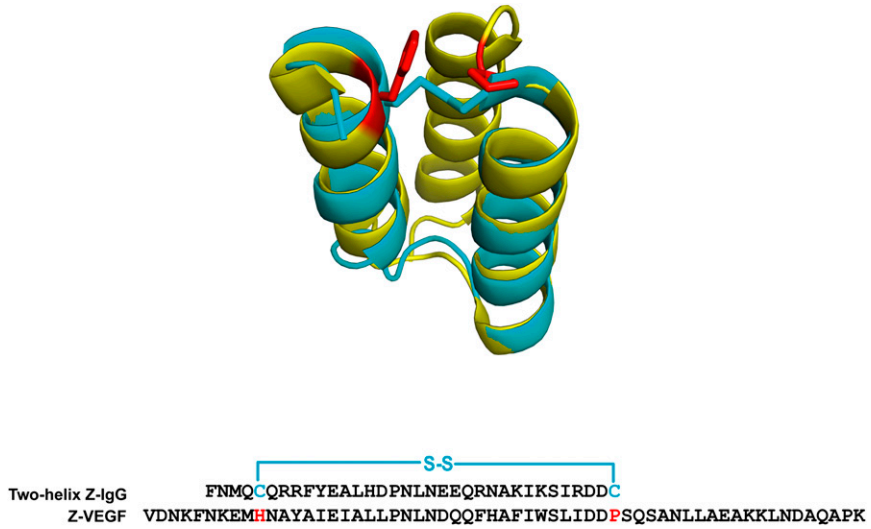

Fig. S3. Overlay of cartoon representation of the crystal structure of Z-VEGF (yellow, from PDB ID code 3S1K) with the NMR solution structure of previously reported two-helix analog of Z-IgG (teal; PDB ID code 1ZDD); disulfide bond is shown as sticks. From inspection of the overlay, location of Cys residues in two-helix Z-IgG appears to correspond well with His^{10} and Pro^{39} of Z-VEGF, highlighted in red.

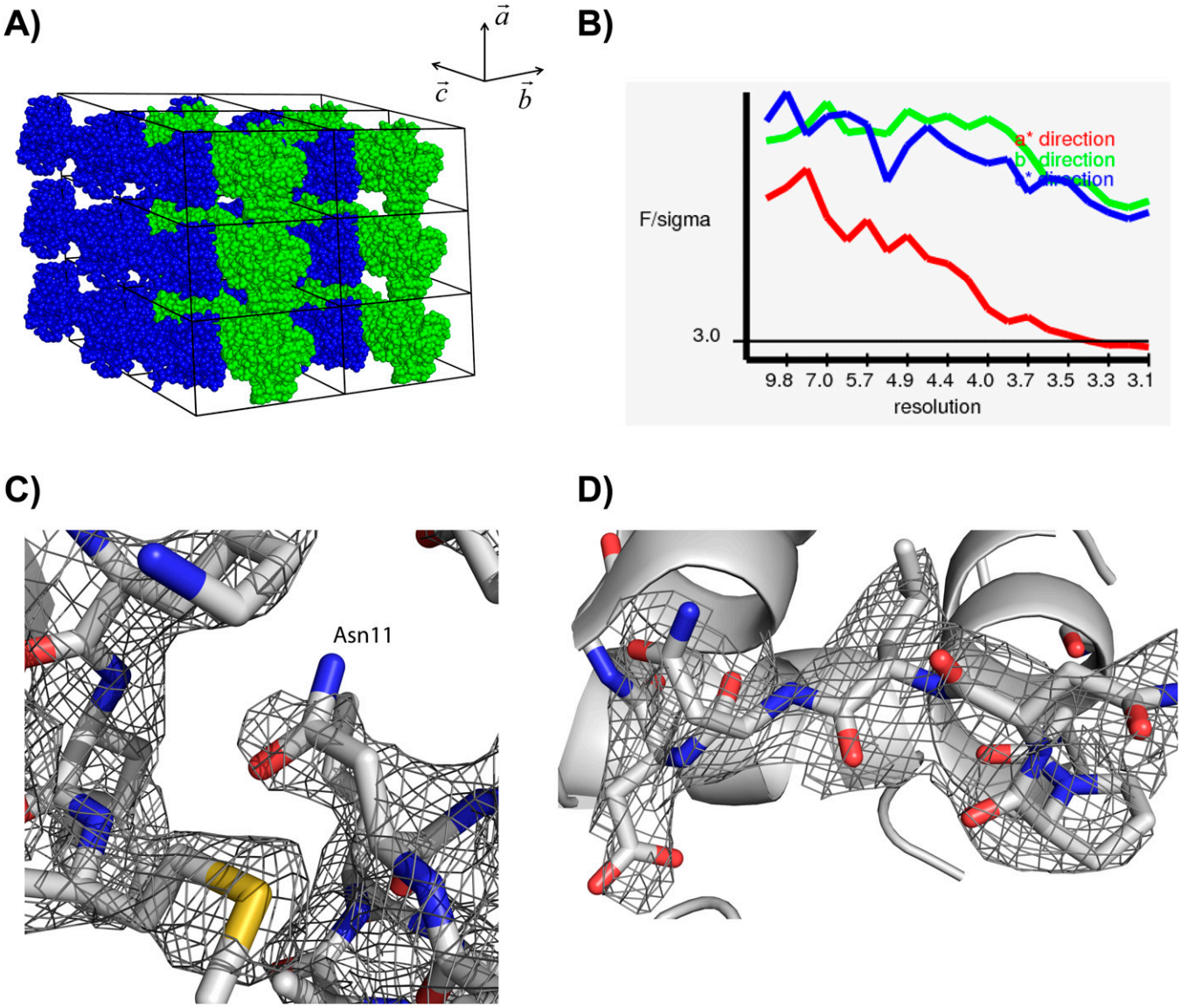

Fig. S4. Crystal structure of α/β-VEGF-1 in complex with $VEGF_{8–109}$. (*A*) A block of 3 × 2 × 2 unit cells that illustrate the crystal packing of $VEGF_{8–109}$ dimers with the α/β-peptide α/β-VEGF-1; crystallographic axes are indicated. (*B*) A graph of $|F_{obs}|/\sigma(|F_{obs}|)$ as a function of resolution, generated by the University of California, Los Angeles–Molecular Biology Institute Diffraction Anisotropy Server (services.mbi.ucla.edu/anisoscale/ and ref. 1). Magnitudes of $|F_{obs}|/\sigma(|F_{obs}|)$ corresponding to reciprocal axes *a**, *b**, and *c** are indicated in red, green, and blue, respectively. (*C*) A contact between the side chain of α/β-VEGF-1 Asn^{11} (chain C) and $VEGF_{8–109}$ (chain A), electron density is represented as a $2mF_o - DF_c$ weighted map contoured at 1.2σ. (*D*) Residues 20–25 within the loop region of α/β-VEGF-1 (DPNLND, chain D); electron density is represented as a $2mF_o - DF_c$ weighted map contoured at 1.2σ.

1. Strong M, et al. (2006) Toward the structural genomics of complexes: Crystal structure of a PE/PPE protein complex from *Mycobacterium tuberculosis*. *Proc Natl Acad Sci USA* 103(21): 8060–8065.

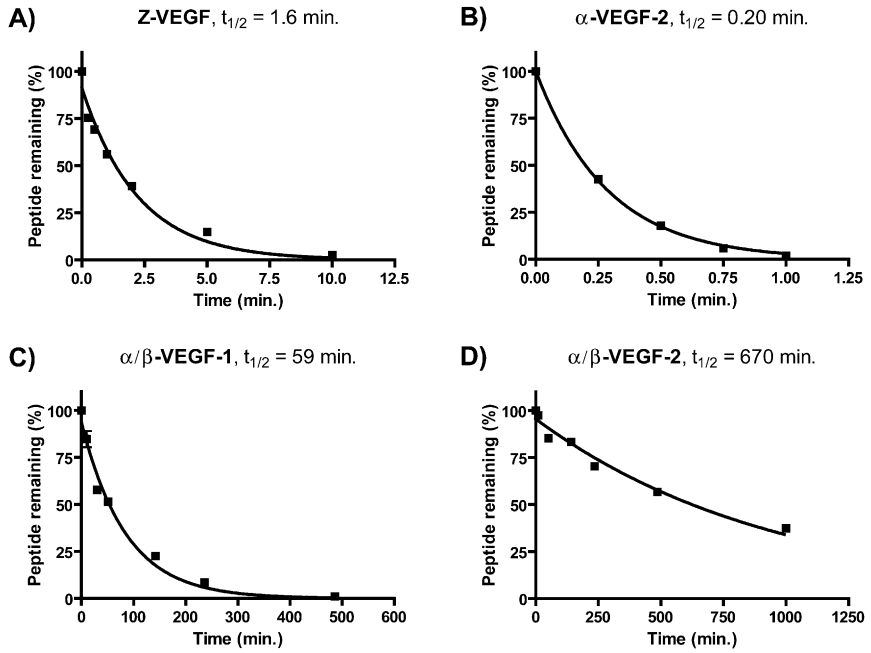

Fig. S5. Time-dependent proteolysis of 45 μM α- or α/β-peptide with 10 μg/mL proteinase K in TBS, pH 7.5, at room temperature. Each data point indicates the mean ± SEM for two independent reactions run in parallel at the indicated time point. Note the different scales on the horizontal axes. (*A*) Proteolysis curve of Z-VEGF ($t_{1/2}$ = 1.6 min). (*B*) Proteolysis curve of α-VEGF-2 ($t_{1/2}$ = 0.20 min). (*C*) Proteolysis curve of α/β-VEGF-1 ($t_{1/2}$ = 59 min). (*D*) Proteolysis curve of α/β-VEGF-2 ($t_{1/2}$ = 670 min).

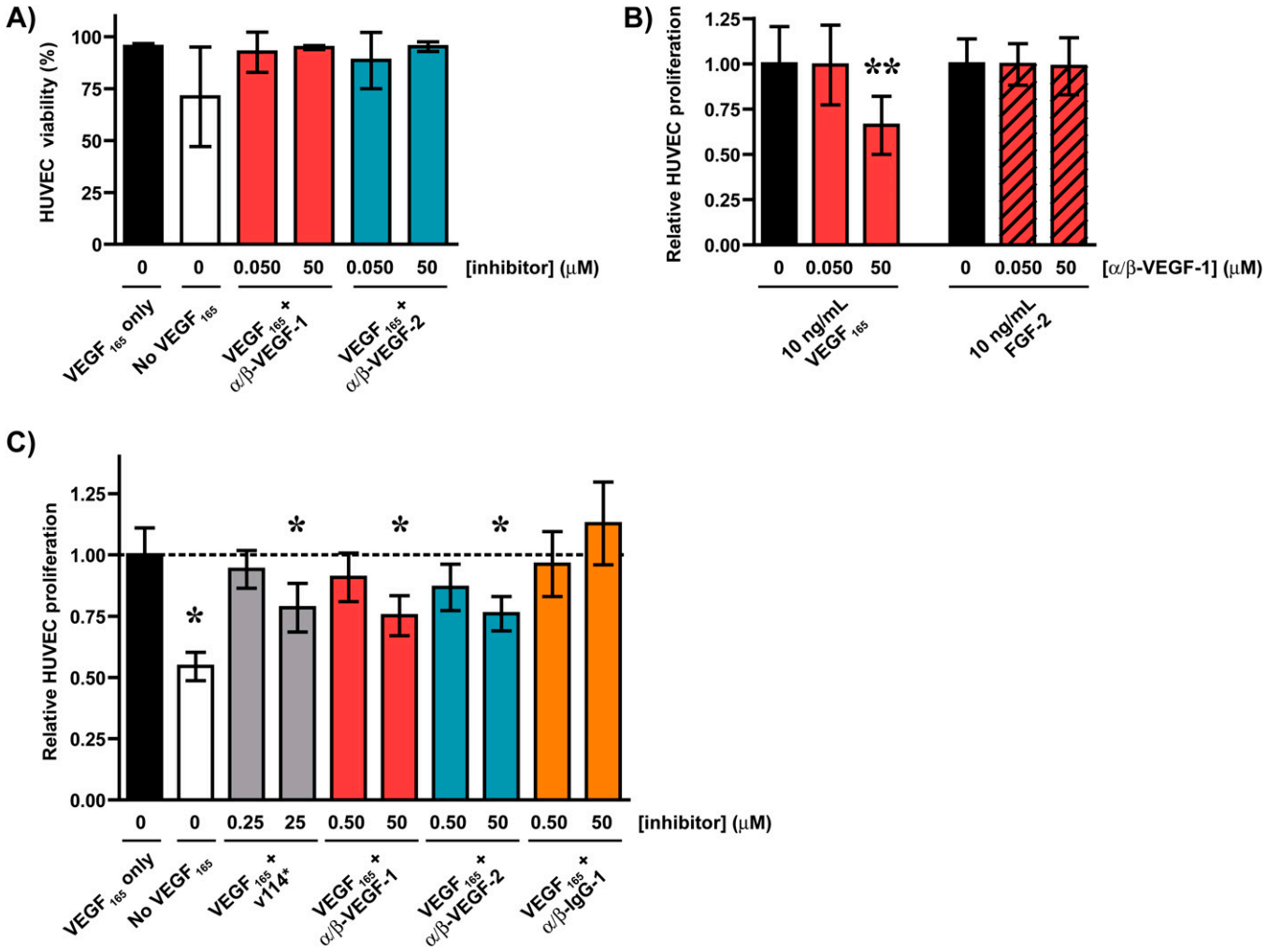

Fig. S6. (*A*) Representative experiment showing the viability of HUVECs treated with 10 ng/mL $VEGF_{165}$ and the indicated concentration of inhibitor, as determined by LIVE/DEAD viability assay (Life Technologies). Columns represent the mean ± SD from $n = 6$ replicate wells for each condition. Statistical comparisons were formed using two-tailed *t* test relative to $VEGF_{165}$ only condition—no significant differences were observed (value of $P > 0.05$). (*B*) Representative experiment showing the relative proliferation of HUVECs treated with 10 ng/mL $VEGF_{165}$ or 10 ng/mL FGF-2 and the indicated concentration of α/β-VEGF-1, as determined by Click-iT EdU assay. Columns represent the mean ± SD from $n = 8$ replicate wells for each condition. Data normalized to the average value for the "0 μM α/β-VEGF-1" control (black bars) for the respective growth factor. Significant differences were denoted for value of $P \leq 0.0125$ (**) relative to respective 0 μM α/β-VEGF-1 control using a two-tailed *t* test. (*C*) Representative experiment showing the relative proliferation of HUVECs treated with 10 ng/mL $VEGF_{165}$ and oligomers at the concentrations indicated. Columns represent mean ± SD from $n = 8$ replicate wells for each experimental condition and $n = 16$ replicate wells for $VEGF_{165}$-only control as measured via Click-iT EdU assay. The sequence of v114* (positive control) is given in *Methods* in the main text (from ref. 1). Values were normalized to the average value of the $VEGF_{165}$-only control (black bar, dotted line). Significant differences within this experiment were denoted for a value of $P \leq 0.0055$ (*) relative to $VEGF_{165}$-only control using a two-tailed *t* test.

1. Haase HS, et al. (2012) Extending foldamer design beyond α-helix mimicry: α/β-Peptide inhibitors of vascular endothelial growth factor signaling. *J Am Chem Soc* 134(18):7652–7655.

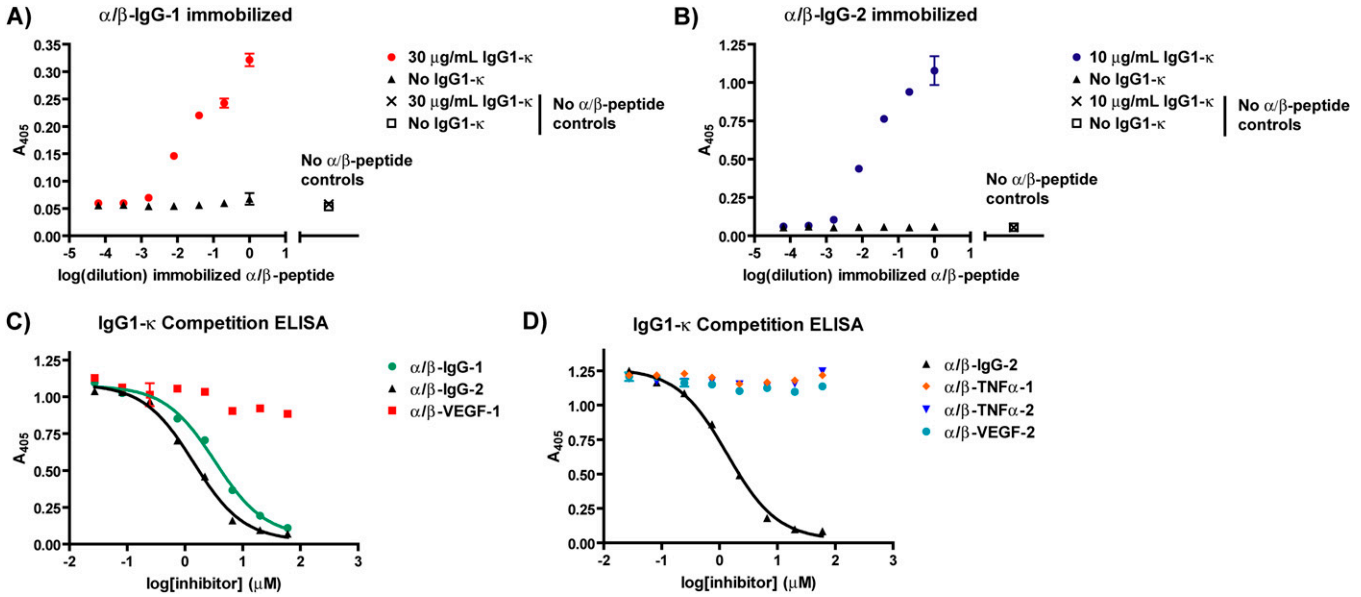

Fig. S7. Indirect ELISA detecting the binding of human IgG1-κ to immobilized α/β-peptide+BSA conjugates (*A*) α/β-IgG-1+BSA conjugate with 30 μg/mL IgG1-κ and (*B*) α/β-IgG-2+BSA conjugate with 10 μg/mL IgG1-κ. Filled circles indicate signal when wells are incubated with respective amount of IgG1-κ. Black triangles indicate signal observed for the given dilution of immobilized α/β-peptide conjugate that is not incubated with IgG1-κ. Points labeled "No α/β-peptide controls" indicate wells incubated with or without IgG1-κ in which no α/β-peptide has been immobilized. Data points represent the mean ± SEM of duplicate wells on the plate. *C* and *D* show IgG1-κ competition ELISA comparing the relative ability of different α/β-peptides to inhibit binding of 10 μg/mL IgG1-κ to immobilized α/β-IgG-2+BSA conjugate. Both *C* and *D* are independent experiments with α/β-IgG-2 used as an inhibitor in both assays to show reproducibility. Data points represent the mean ± SEM of duplicate wells on plate.

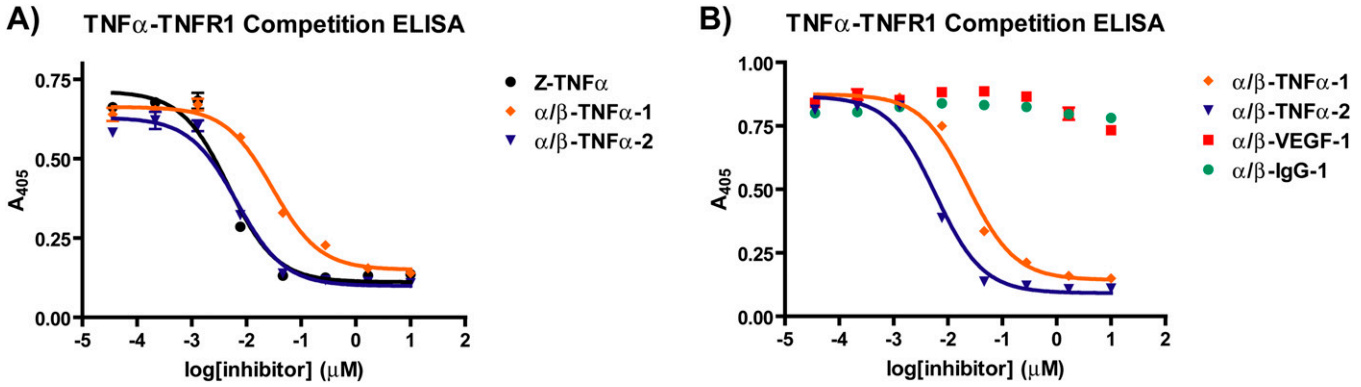

Fig. S8. Representative competition ELISA experiments evaluating the ability of oligomers Z-TNFα (*A*), α/β-TNFα-1 (*A* and *B*), α/β-TNFα-2 (*A* and *B*), α/β-VEGF-1 (*B*), and α/β-IgG-1 (*B*) to block the binding of TNFα to immobilized TNFR1. Each panel represents an independent experiment with some oligomers present on multiple plates as positive controls and to show reproducibility. Data points represent the mean ± SEM from duplicate wells on plate.

Table S1. X-ray data collection and refinement statistics and parameters

Data collection	
X-ray source	APS 21-ID-F
X-ray detector	MAR225
Wavelength, Å	0.97872
Space group	$P2_1$
a/*b*/*c*, Å	39.1/78.4/56.5
β, °	102.8
Volume, Å^3	169,000
Matthews coefficient, Å^3/Da	2.56
Solvent content, %	51.9
Molecules per asymmetric unit	4
Resolution range, Å*	45.08–3.11 (3.22–3.11)
No. of observations	22,104 (2,325)
Unique reflections	6,038 (616)
Completeness	99.6% (100%)
Redundancy	3.7 (3.8)
Mean $I/\sigma(I)$	14.2 (7.6)
$CC_{1/2}$	0.995 (0.978)
Wilson *B* factor, Å^2	44.0
R_{merge}	0.083 (0.233)
R_{meas}	0.097 (0.272)
R_{pim}	0.050 (0.139)
Refinement statistics	
Refinement program	*phenix.refine*: 1.9_1692
Nonhydrogen protein atoms refined	1,909
Resolution range, Å	45.08–3.11 (3.42–3.11)
No. of reflections used in refinement	6,017 (1,492)
Completeness, %	99.3 (99)
Reflections in cross-validation set	506
R value, work, %	24.1 (26.8)
R value, free, %	29.8 (36.1)
R value, overall, %	24.5
Overall mean ADP, Å^2	66.8
Coordinate error, ML, Å	0.41
RMSD	
Bond lengths, Å	0.025
Bond angles, °	1.475

*Highest resolution shell shown in parentheses.